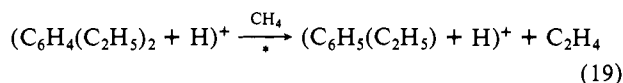
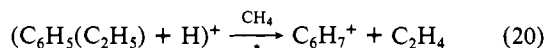


The CI ion chromatogram contains the usual CH_4 CI ions: predominantly protonated diethylbenzene and smaller amounts of $(\text{M} - \text{H})^+$, $(\text{M} + \text{C}_2\text{H}_5)^+$, and $(\text{M} + \text{C}_3\text{H}_5)^+$. The HPCA spectra contain several fragment ions diagnostic of the structure of the sample with the major dissociation pathways being



and



HPCA mass spectra acquired at a fixed extent of dissociation cannot provide the detailed structural information obtained from a breakdown curve. However, when combined with the CI mass spectra and GC retention times, the HPCA data provide a potentially powerful additional dimension in sample characterization.

Acknowledgment is made to the donors of the Petroleum Research Fund, administered by the American Chemical Society, for support of this research.

Registry No. CH_4 , 74-82-8; C_2H_6 , 74-84-0; ethyl acetate, 141-78-6; 3-heptanone, 106-35-4; *o*-dichlorobenzene, 95-50-1; *m*-dichlorobenzene, 541-73-1; ethylbenzene, 100-41-4; *m*-xylene, 108-38-3; *p*-xylene, 106-42-3.

EPR Evidence on Molecular and Electronic Structure of Nitrogen Trifluoride Radical Cation

Alvin M. Maurice,[†] R. Linn Belford,^{*†} Ira B. Goldberg,^{*†} and Karl O. Christe[§]

Contribution from the School of Chemical Sciences, University of Illinois, Urbana, Illinois 61801, Rockwell International Science Center, Thousand Oaks, California 91360, and Rocketdyne Division, Rockwell International, Canoga Park, California 91304. Received April 26, 1982

Abstract: Computer simulations of the EPR spectra of rigid $^{14}\text{NF}_3^+$ and $^{15}\text{NF}_3^+$ trapped in powdered NF_4AsF_6 at 25 K show characteristics of a trigonal pyramid with the following principal values for the coupling matrices: $|g(\parallel, \perp)| = 2.003$; $|A_{15\text{N}}(\parallel, \perp)| = 324, 187$ MHz; $A_{15\text{N}}(\parallel, \perp) = 451, 260$ MHz; $A_{19\text{F}}(z, x, y) = 880, 340, 360$ MHz; α , the angle between parallel axes for $A_{19\text{F}}$ and $A_{15\text{N}} = 15^\circ$. The nitrogen p:s spin-density ratio (computed from the nitrogen hyperfine splittings) is consistent with $\text{sp}^{2.5}$ nitrogen hybrids in the NF bonds and with a pyramid angle of about 105° . Although the same pyramid angle appears to agree with the orientation of the principal axis of the fluorine hyperfine coupling matrix ($|\alpha| = 15^\circ$, pyramid angle = $90^\circ + |\alpha|$), electronic structure computations imply that α is negative and that the agreement is fortuitous. Some comparisons are made with isoelectronic radicals BF_3^- and CF_3^- —the latter being essentially tetrahedral with sp^3 hybridization.

Goldberg, Crowe, and Christe have presented high- and low-temperature EPR spectra of the radical cations $^{14}\text{NF}_3^+$ and $^{15}\text{NF}_3^+$ produced by γ -irradiation of NF_4AsF_6 .¹ Their analyses properly accounted for the high-temperature (~ 240 K) spectra, but computational limitations prevented a complete analysis of the low-temperature (~ 25 K) EPR spectra, which are drastically different. At the high temperature, the molecule is axially symmetric, apparently spinning freely, probably both about its threefold axis and about an axis nearer to the F_3 plane. In contrast, at the low temperature, each molecule appears to be locked into a fixed orientation and the EPR spectra are, as expected, much more complex. Now, with an appropriately modified computer simulation program, we are able to interpret these low-temperature spectra.

Several studies providing information on hyperfine coupling, spin density, and geometry of the isoelectronic species BF_3^{2-} and CF_3^- have been published.³⁻⁷ The opportunity to compare those bonding features that can be deduced from hyperfine matrices of the isoelectronic series provides one of the motivations for the study of NF_3^+ . Here we describe our interpretation of the low-temperature EPR spectra and draw conclusions regarding geometry and bonding in the nitrogen trifluoride radical cation.

Experiments and Computation

Low-temperature EPR spectra of $^{14}\text{NF}_3^+$ and $^{15}\text{NF}_3^+$ have been described¹ as have the synthesis, experimental conditions, and the spectrometer used in this work. The spectra chosen for the current analysis are reproduced in the figures.

Simulated EPR spectra are generated by means of the program "POWD" running on the VAX 11/780 computer connected to a Houston Instruments HIPLLOT digital plotter. Program POWD has its origins in an EPR powder simulation program, kindly provided by Dr. J. R. Pilbrow of Monash University, which employs second-order perturbation theory for the first nucleus and first-order approximations for superhyperfine terms. It was revised by White and Belford^{8,9} and Chasteen et al.¹⁰ into EPRPOW. Nilges and Belford^{11,12} rewrote this program as POW to employ more efficient angular sampling (to minimize the unevenness of point density on the sphere) and integration technique four-point Gauss quadrature.¹³ The version of POWD that we have created for the current work is a substantially modified POW that uses a perturbation method accurate to second order in all hyperfine terms (including internuclear cross-terms)¹⁴ to calculate a powder spectrum for a spin $S = 1/2$ system with up to four hyperfine nuclei. Program POWD permits principal axes of all four hyperfine nuclei interaction matrices as well as those of the

- (1) I. B. Goldberg, H. R. Crowe, and K. O. Christe, *Inorg. Chem.*, **17**, 3189 (1978).
- (2) R. L. Hudson and F. Williams, *J. Chem. Phys.*, **65**, 3381 (1976).
- (3) R. W. Fessenden, *J. Magn. Reson.*, **1**, 277 (1969).
- (4) R. W. Fessenden and R. H. Schuler, *J. Chem. Phys.*, **43**, 2704 (1965).
- (5) M. T. Rogers and L. D. Kispert, *J. Chem. Phys.*, **46**, 3193 (1967).
- (6) J. Maruani, J. A. R. Coope, and C. A. McDowell, *Mol. Phys.*, **18**, 165 (1970).
- (7) J. Maruani, C. A. McDowell, H. Nakajima, and P. Raghunathan, *Mol. Phys.*, **14**, 349 (1968).
- (8) L. K. White and R. L. Belford, *J. Am. Chem. Soc.*, **98**, 4428 (1976).
- (9) L. K. White, Ph.D. Thesis, University of Illinois, Urbana, 1975.
- (10) N. F. Albanese and N. D. Chasteen, *J. Phys. Chem.*, **82**, 910 (1978).
- (11) M. J. Nilges and R. L. Belford, *J. Magn. Reson.*, **35**, 259 (1975).
- (12) M. J. Nilges, Ph.D. Thesis, University of Illinois, Urbana, 1979.
- (13) R. L. Belford and M. J. Nilges, "Computer Simulation of EPR PowderSpectra", Symposium on Electron Paramagnetic Resonance Spectroscopy, Rocky Mountain Conference on Analytical Chemistry, Denver, August 1979.
- (14) J. A. Weil, *J. Magn. Reson.*, **18**, 113 (1975).

[†]University of Illinois.

^{*}Rockwell International Science Center.

[§]Rocketdyne Division.

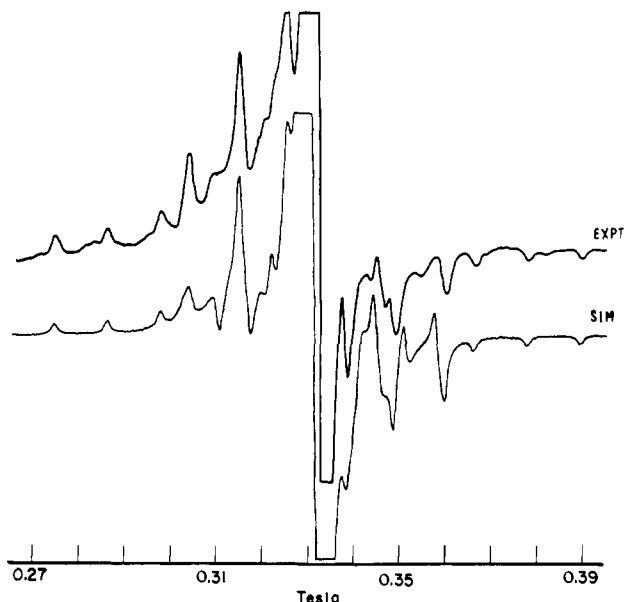


Figure 1. (EXPT) EPR spectrum of $^{14}\text{NF}_3^+$ at 26 K in $\text{NF}_4\text{A}_5\text{F}_6$ γ -irradiation at 77 K after annealing at 195 K. (SIM) $^{14}\text{NF}_3^+$ computer simulation with the parameters listed in Table I.

g tensor to be noncoincident. For this computation, all nuclear Zeeman and quadrupole terms are deemed insignificant and are ignored.

Theory

The Hamiltonian is

$$\mathcal{H}_s = \beta \vec{S} \cdot \vec{g} \cdot \vec{B} + \sum_{i=1}^3 \vec{I}_i \cdot \vec{A}_i \cdot \vec{S}$$

which generates the following energy terms, correct to the second order of perturbation:⁴

$$E(M, m_1, m_2, m_3, m_4) = g\beta B M_S + \left[K_1 M_s m_1 + \frac{M_s}{2g\beta B} \left\{ \frac{1}{2} (\text{tr}(\vec{A}_1 \cdot \vec{A}_1) - k_1^2) \cdot \left(\frac{1}{2} \right) (I_1 \langle I_1 + 1 \rangle - m_1^2) \right\} \right] + \left[K_2 M_s m_2 + \frac{M_s}{2g\beta B} \left\{ \frac{1}{2} (\text{tr}(\vec{A}_2 \cdot \vec{A}_2) - k_2^2) \left(\frac{1}{2} \right) \times (I_2 \langle I_2 + 1 \rangle - m_2^2) \right\} \right] + \dots + \frac{1}{2g\beta B} \left[\left\{ -\frac{\text{Det}(A_1)}{K_1} \left(\frac{1}{2} \right) m_1 + (k_1^2 - K_1^2) M_s m_1^2 \right\} + \left\{ -\frac{\text{Det}(A_2)}{K_2} \left(\frac{1}{2} \right) m_2 + (k_2^2 - K_2^2) M_s m_2^2 \right\} + \dots \right] + \frac{M_s}{2g\beta B} [(L_{12} - K_1 K_2) m_1 m_2 + (L_{13} - K_1 K_3) m_1 m_3 + (L_{14} - K_1 K_4) m_1 m_4 + (L_{23} - K_2 K_3) m_2 m_3 + (L_{24} - K_2 K_4) m_2 m_4 + (L_{34} - K_3 K_4) m_3 m_4]$$

where

$$g^2 \equiv \vec{\eta} \cdot \vec{g} \cdot \vec{g} \cdot \vec{\eta}$$

$$g^2 K_1^2 \equiv \vec{\eta} \cdot \vec{g} \cdot \vec{A}_1 \cdot \vec{A}_1 \cdot \vec{g} \cdot \vec{\eta}$$

$$g^2 K_1^2 k_1^2 \equiv \vec{\eta} \cdot \vec{g} \cdot \vec{A}_1 \cdot \vec{A}_1 \cdot \vec{A}_1 \cdot \vec{A}_1 \cdot \vec{g} \cdot \vec{\eta}$$

$$g^2 K_1 K_2 L_{12} \equiv \vec{\eta} \cdot \vec{g} \cdot \frac{1}{2} (\vec{A}_1 \cdot \vec{A}_1 \cdot \vec{A}_2 \cdot \vec{A}_2 + \vec{A}_2 \cdot \vec{A}_2 \cdot \vec{A}_1 \cdot \vec{A}_1) \cdot \vec{g} \cdot \vec{\eta}$$

These terms are used in POWD to construct transition energies from which transition fields are computed by an approximation to the

Table I. Hyperfine Matrices^a and g Values of $^{14}\text{NF}_3^+$ and $^{15}\text{NF}_3^+$.

	$^{14}\text{NF}_3^+$	$^{15}\text{NF}_3^+$
$A_N(\perp)$	(+) 187.1 ± 5.0^b	(-) 259.5 ± 7
$A_N(\parallel)$	(+) 324.3 ± 1.4	(-) 450.8 ± 2
$A_F(x)$	(\pm) 340.0 ± 20	(\pm) 340.0 ± 20
$A_F(y)$	(\pm) 360.0 ± 20	(\pm) 360.0 ± 20
$A_F(z)$	(\pm) 880.0 ± 1	(\pm) 880.0 ± 1
$g(\perp)$	2.002	2.002
$g(\parallel)$	2.001	2.001
α	$15.0 \pm 1^\circ$	$15.0 \pm 1^\circ$

^a Hyperfine splittings are in MHz. ^b Uncertainties were estimated by comparing numerous simulations to the experimental spectra. The estimates given are ranges outside which, in our subjective judgment, a satisfactory fit to the spectra could not be achieved.

first-order frequency shift perturbation formula.¹⁵

Low-Temperature Spectrum of $^{14}\text{NF}_3^+$. The overall shape of the experimental EPR spectrum (see Figure 1) does not match our preliminary computer simulations. The comparisons suggest that the experimental spectrum contains a spurious component—a broad background. The EPR spectra of BF_3^{-2} exhibited a similar background, which was attributed to a matrix radical ($\cdot\text{CH}_2\text{SiMe}_3$). Accordingly, a background curve consisting of a single, broad peak was included for all simulations of NF_3^+ . A word of caution is in order. Even though we had to include an extra background peak to accomplish the analysis, we cannot prove that it is not part of the spectrum of the species under study. To avoid any further arbitrariness, we allowed this background to have no structure. The necessity for including a superimposed background spectrum introduces extra uncertainty in the parameters, especially the perpendicular peaks that are located where the background is most intense. Because the hyperfine splitting is larger for parallel peaks, these peaks are masked to a lesser degree.

The additional uncertainty introduced by the background spectrum is somewhat compensated for by the availability of spectra for two different nitrogen isotopes. The ground rules for simulation of the two isotopic species are as follows. Both spectra should be defined by identical g matrices and fluorine hyperfine matrices and angle α . (Note: α is the angle between the principal axes of the ^{19}F and N hyperfine matrices; it may be close to the angle between the N-F bond and the plane of the three fluorines (see Figure 3 and Discussion).) The nitrogen hyperfine matrix elements should be related by a factor of -1.4029 , which is the ratio of their nuclear moments (i.e., $A_\perp(^{15}\text{N})/A_\perp(^{14}\text{N}) = A_\parallel(^{15}\text{N})/A_\parallel(^{14}\text{N}) = -1.4029$). Fitting two isotopic spectra with the same parameters in this way increases our confidence in the resulting values.

Low-Temperature Spectrum of $^{15}\text{NF}_3^+$. Similarly, the $^{15}\text{NF}_3^+$ experimental spectrum (see Figure 2) also suggests a broad background resonance, which was included in the simulations.

Discussion

The principal values of the hyperfine and g matrices for both isotopes are listed in Table I. One can estimate the spin density of the free electron from the nitrogen hyperfine parameters obtained from the $^{14}\text{NF}_3^+$ simulation and the equations in the article by Goldberg et al.:¹

$$\rho^s_{\text{N}} = a_{\text{N}}(\text{iso})/a^\circ_{\text{N}} \quad \rho^p_{\text{N}} = (A_{\text{N}}(\parallel) - a_{\text{N}}(\text{iso}))/2b^\circ_{\text{N}}$$

In these equations ρ^s_{N} and ρ^p_{N} are integrated spin densities of the s and p orbitals; a°_{N} and b°_{N} are the reference atomic isotropic and anisotropic hyperfine couplings,¹⁶ respectively. The calculated ratio of ρ^p_{N} to ρ^s_{N} , 6.37, suggests the unpaired electron to be largely in the following hybrid orbitals:

$$\psi_1 = 0.9293\psi_{\text{N}}(2p_z) + 0.3694\psi_{\text{N}}(2s)$$

(15) R. L. Belford, P. H. Davis, G. G. Belford, T. M. Lenhart, *ACS Symp. Ser.*, No. 5 (1974).

(16) J. E. Wertz and J. R. Bolton, "Electron Spin Resonance: Elementary Theory and Practical Applications", McGraw-Hill, New York, 1972.

Table II. Comparison of Hyperfine Couplings^a and Spin Densities^b of MF_3 Radicals

	$ A_{\text{M}}(x) $	$ A_{\text{M}}(y) $	$ A_{\text{M}}(z) $	$a_{\text{M}}(\text{iso})$	$ A_{\text{F}}(x) $	$ A_{\text{F}}(y) $	$ A_{\text{F}}(z) $	$a_{\text{F}}(\text{iso})$	$\rho_{\text{M}}^{\text{S}}$	$\rho_{\text{M}}^{\text{P}}$	$\rho_{\text{F}}^{\text{S}}$	$\rho_{\text{F}}^{\text{P}}$	hybridization of M-F bond
BF_3^-				428.7 ^c				498.8 ^c	0.211		0.0104		
CF_3^-	667.7 ^d	720.8 ^d	891.2 ^d	759.9 ^d	258.1 ^d	246.8 ^d	709.1 ^d	404.7 ^d	0.244	0.723	0.0084	0.1113	$\text{sp}^{3.01}$
CF_3^-					244.1 ^e	224.4 ^e	738.5 ^e	402.3 ^d					
NF_3^+	187.1 ^f	187.1 ^f	324.3 ^f	232.8 ^f	340.0 ^f	360.0 ^f	880.0 ^f	526.7 ^f	0.151 (0.129)	0.957 (0.824)	0.0110	0.1166	$\text{sp}^{2.47}$

^a Hyperfine splittings are in MHz. ^b Spin densities are calculated from hyperfine values as in ref 1 and 16; those in parentheses are calculated from the newer compilation by: J. R. Morton and K. F. Preston, *J. Magn. Reson.* 30, 577 (1978). ^c See ref 2. ^d See ref 5. ^e See ref 6 and 7. ^f This work.

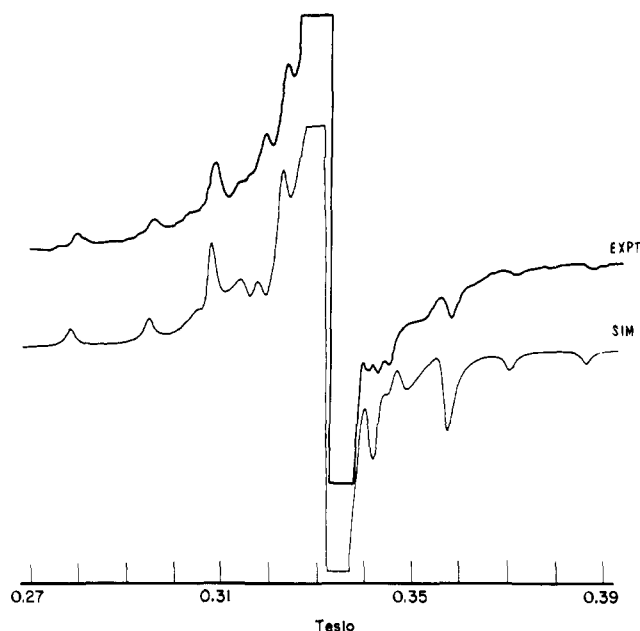


Figure 2. (EXPT) EPR spectrum at $^{15}\text{NF}_3^+$, at 24 K in $^{15}\text{NF}_4\text{A}_3\text{F}_6$ γ -irradiated at 77 K after annealing at 195 K. (SIM) $^{15}\text{NF}_3^+$ computer simulation generated by the program POWD with the variables listed in Table I. See text.

having about 13.6% s and 86.4% p character. A simplified hybrid orbital picture of the bonding in NF_3^+ can then be constructed in the following way. Starting with an isolated $^5\text{S N}^+$ ion (prepared for bonding with four valence electrons in four orbitals—one s and three p ($2s^{\uparrow}, 2p^{\uparrow\uparrow\uparrow}$)) and eliminating the singly occupied nonbonding $s^{0.136}p^{0.864}$ orbital from the s and 3p's leaves 0.8635 s and 2.1365 p—that is, three N-F bonds, each using a nitrogen hybrid $s^{0.2878}p^{0.7122}$ or ca. $\text{sp}^{2.5}$. Now it is interesting to predict the angle, α' , between $\text{sp}^{2.5}$ orbitals and the plane of the 3 F atoms¹⁷ and compare it with the angle α , which characterizes the ^{19}F hyperfine interaction anisotropy.

The four N^+ bonding electrons must be placed in four orthogonal orbitals, the nonbonding one directed along the z axis (ψ_1) and three equivalent ones (ψ_2, ψ_3, ψ_4) directed along the N-F bonds. It is sufficient to consider any one of the bonding orbitals, ψ_2 , chosen to be directed somewhere in the xz plane (Figure 3). Orthonormality requires $\langle \psi_1, \psi_2 \rangle = 0$ and

$$\psi_1 = (1 - 3f)^{1/2}\psi_{\text{N}}(2s) + (3f)^{1/2}\psi_{\text{N}}(2p_z)$$

$$\psi_2 = f^{1/2}\psi_{\text{N}}(2s) + (1 - f)^{1/2}\psi_{\text{N}}(2p_z) = f^{1/2}\psi_{\text{N}}(2s) + (1 - f)^{1/2}[-\cos \lambda \psi_{\text{N}}(2p_z) + \sin \lambda \psi_{\text{N}}(2p_x)]$$

where the f is the fraction of s character in the nitrogen bonding orbital ψ_2 . With $3f^{1/2} = 0.9293$ as previously estimated, we find $\cos \lambda = 0.2527$, or $\lambda = 75.4^\circ$, $\alpha' = 14.6^\circ$. The angle between

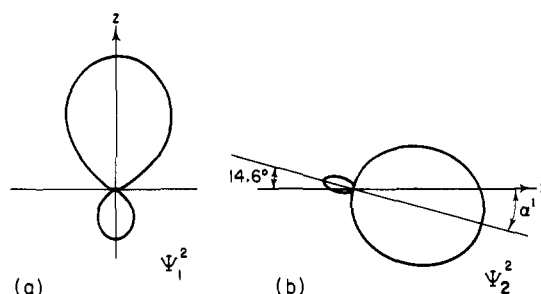


Figure 3. (a) Nonbonding orbital directed along the z axis, ψ_1 . This orbital is a linear combination of a nitrogen 2s and $2p_z$ orbital. (b) One of the three nitrogen bonding orbitals. This orbital is in the xz plane and is directed along the N-F bond.

any NF bond and the threefold axis might be expected to be about 104.6° , a little under the tetrahedral angle (109.5°).

It is interesting that the magnitude of α' agrees with the value of $|\alpha| = 15 \pm 1^\circ$ (Table I). The consistency in magnitude between the isotropic and dipolar nitrogen hyperfine matrix and the dipolar fluorine hyperfine matrix within a simple hybrid-orbital picture of bonding is remarkable. However, since the experiment and simulations provide only the magnitude of α and not its sign, the agreement could be illusory. A similar, generally consistent picture can be constructed for $\cdot\text{CF}_3$, which was previously analyzed. For this radical, the magnitude of α was 17.8° , and judging from the ^{13}C hyperfine matrices, it has a consistent hybridization of $\sim\text{sp}^3$; more specifically, $\alpha' = 19.6^\circ$; Edlund et al.¹⁸ propose, on the basis of INDO calculations, that the measured value of α is actually -17.8° . That is, they assert that, fortuitously, the spin-density distribution is such that α and α' are approximately equal in magnitude but opposite in sign, making a large angle ($\sim 37^\circ$) between the principal axis of the fluorine hyperfine matrix and the normal to the C-F bond. With no more information, it is difficult to judge the validity of their conclusion, particularly as INDO methods are grounded in a great many formidable approximations. However, since Edlund et al. supplemented their INDO work with a few ab initio computations, with similar results, one must suspect that α really is negative for $\cdot\text{CF}_3$ and possibly for $\cdot\text{NF}_3^+$ and/or $\cdot\text{BF}_3^-$ as well. Therefore, Benzal et al.¹⁹ have carried out full ab initio computations, with geometric variation to establish the potential minima, on the isoelectronic series $\cdot\text{NF}_3^+$, $\cdot\text{CF}_3$, and $\cdot\text{BF}_3^-$. The results, presented in the following paper, generally confirm the proposition of Edlund et al.¹⁸ They support the idea that the main fluorine contribution to the singly occupied molecular orbital (HOMO) is a p orbital that is directed along the principal axis of the ^{19}F hyperfine coupling matrix but that is neither coincident with nor orthogonal to any of the bonds or molecular symmetry axes. The anisotropic part of the fluorine hyperfine coupling apparently can indicate the spin density and orientation of this participating p orbital but cannot be used to establish the molecular geometry.

(18) O. Edlund, A. Lund, M. Shiotani, J. Sohma, and K. A. Thuomus, *Mol. Phys.*, 31, 49 (1976).

(19) M. Benzal, A. M. Maurice, R. L. Belford, and C. E. Dykstra, *J. Am. Chem. Soc.*, following paper in this issue.

(17) C. A. Coulson, "Valence", Oxford University Press, London, 1961.

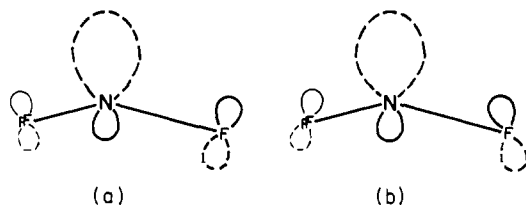


Figure 4. Schematic representation of the two possible local orbital schemes for the highest (singly) occupied molecular orbital in $\text{NF}_3^{\bullet+}$; (a) F orbital essentially orthogonal to bond direction, $\alpha = +15^\circ$; (b) F orbital tilted toward bond direction, $\alpha = -15^\circ$.

Conclusions

Despite an apparently large, diffuse background, it has been possible to obtain satisfactory Zeeman, nitrogen hyperfine, and fluorine hyperfine matrices for the rigid trigonal-pyramidal $\cdot\text{NF}_3^+$ radical cation by computer simulation of the EPR spectra of λ -irradiated NF_4AsF_6 and $^{15}\text{NF}_4\text{AsF}_6$, annealed and then cooled to ~ 25 K.

All the data can be rationalized in terms of a hybrid-orbital bonding scheme with (1) the unpaired electron in mainly a non-bonding $\text{N}(\text{sp}^{6.35})$ orbital (which also to some extent involves fluorine p_z orbitals in an antibonding interaction), (2) $\text{sp}^{2.5}$ nitrogen hybrid bonding orbitals, (3) 105° angles between the threefold

axis and the N-F bonds, and (4) the fluorine part of the HOMO being mainly p_z -like, with its z axis tilted plus or minus 15° from the threefold axis (see Figure 4).

The isoelectronic radical $\cdot\text{CF}_3$ is similar, the corresponding angle being 108° and the carbon bonding hybrids about sp^3 (see Table II). Unfortunately, no anisotropic data are available for BF_3^- , the next member of the isoelectronic series; isotropic parameters are compared in Table II.

The structural angles between the C_3 axis and normals to the bonds for $\cdot\text{NF}_3^+$ and $\cdot\text{CF}_3$ are $\sim 14.6^\circ$ and 19.6° , respectively. The principal axes of the fluorine hyperfine matrices deviate from the C_{3v} axes by $\sim 15^\circ$ and 18° , respectively. Depending on the sign of this deviation, these fluorine A axes could be either essentially perpendicular to or tilted, by $\sim 30^\circ$ or 37° , respectively, from the N-F or C-F bonds. The latter interpretation (schematically indicated in Figure 4b) is supported by electronic structure calculations.

Acknowledgment. This work was in part supported by the National Science Foundation Quantum Chemistry Program, the U.S. Army Research Office, and the Office of Naval Research. We thank Mary Kolor Gurnick for helpful suggestions.

Registry No. $^{14}\text{NF}_3^+$, 54384-83-7; $^{15}\text{NF}_3^+$, 67745-75-9; NF_4AsF_6 , 16871-75-3.

Ab Initio SCF Study of Hyperfine Couplings, Geometries, and Inversion Barriers in the Isoelectronic Radicals NF_3^+ , CF_3 , and BF_3^-

M. A. Benzel, A. M. Maurice, R. L. Belford,* and C. E. Dykstra*

Contribution from the School of Chemical Sciences, University of Illinois, Urbana, Illinois 61801. Received April 26, 1982

Abstract: Ab initio SCF molecular orbital calculations with double- ζ and polarized double- ζ bases are reported for the isoelectronic series of C_{3v} radicals $\cdot\text{NF}_3^+$, $\cdot\text{CF}_3$, and $\cdot\text{BF}_3^-$. At the potential minima, the bond lengths are 1.314 Å for NF_3^+ , 1.341 Å for CF_3 , and 1.442 Å for BF_3^- ; the complements of the umbrella angles are $+12.1^\circ$ for NF_3^+ , $+17.1^\circ$ for CF_3 , and $+19.6^\circ$ for BF_3^- . Calculated inversion barriers are about 11, 33, and 28 kcal/mol for NF_3^+ , CF_3 , and BF_3^- , respectively. Bonding and the predicted dependence of EPR parameters upon radical geometry are discussed. With respect to the spin-density distribution and the radical geometry, these calculations confirm the general inferences drawn from the previous EPR analysis—in particular, the hyperfine interaction of the central atom. However, an experimental ambiguity in orientation of the principal axis of the fluorine hyperfine coupling matrix is resolved in favor of the nonintuitive alternative. It is concluded that quantitative information about the geometry of such radicals cannot be inferred from the orientation of the halogen hyperfine axes.

The trigonal-pyramidal fluorocarbon $\cdot\text{CF}_3$ and its isoelectronic neighbors $\cdot\text{NF}_3^+$ and $\cdot\text{BF}_3^-$ are archetypal fluoro radicals. However, there have been no direct determinations of the molecular structure of any of these species, and experimental information bearing on their electronic structure is still being accumulated.¹ The most detailed experimental clues available on these species are to be found in the anisotropic electron paramagnetic resonance spectra of $\cdot\text{YM}_3$ ($Y = \text{C}, \text{N}^+, \text{B}^-$) as impurity sites in solids at low temperature. An intriguing feature of both $\cdot\text{CF}_3$, whose EPR parameters are fairly well-known, and $\cdot\text{NF}_3^+$, for which anisotropic EPR results are just now being reported,¹ is that the angle α between the trigonal axis and the principal axis of the ^{19}F hyperfine coupling tensor is about the same as the structural angle α' by the pyramid is expected to deviate from a planar structure. The obvious interpretation is that the part

of the spin density localized on the fluorine center occupies a $p\pi$ orbital oriented perpendicular to the bond. However, since the experiments were done on isotropic (polycrystalline) samples, the relative signs of α and α' are indeterminable. If they are of opposite sign, the obvious interpretation is invalid. In that event, it would seem that the fluorine p orbital involved in the highest (singly occupied) molecular orbital would be poised for bonding by being strongly skewed with respect to the Y-F ($Y = \text{C}, \text{B}^-$, or N^+) bond. In the case of $\cdot\text{CF}_3$, INDO calculations and limited ab initio calculations² have supported this second interpretation. Here we report ab initio self-consistent-field (SCF) calculations with large basis sets, carried out to determine not only the equilibrium structures of the three radicals but also their inversion barriers. These calculations provide detailed information on the electron-spin distributions leading to an elucidation of the rela-

(1) A. M. Maurice, R. L. Belford, I. B. Goldberg, and K. O. Christe, *J. Am. Chem. Soc.*, preceding paper in this issue.

(2) O. Edlund, A. Lund, M. Shiotani, J. Sohma, and K. A. Thuomas, *Mol. Phys.*, **32**, 49 (1976).